Research Square

Preprints are preliminary reports that have not undergone peer review.
They should not be considered conclusive, used to inform clinical practice,
or referenced by the media as validated information.

Brazing of transparent polycrystalline Al2O3 and GH99 with the assistance of (Cu, Ni) solid solution cladding layer

Bo Zhang
Harbin Institute of Technology
Lixia Zhang (hitzhanglixia@163.com)
Harbin Institute of Technology
Zhan Sun
Harbin Institute of Technology
Jicai Feng
Harbin Institute of Technology

Research Article

Keywords: transparent ceramics, alumina, brazing, solid solution, interfaces

Posted Date: March 24th, 2020

DOI: https://doi.org/10.21203/rs.3.rs-18928/v1

License: This work is licensed under a Creative Commons Attribution 4.0 International License.
Read Full License

Abstract

In this study, pure Cu foil was firstly vacuum cladding on the GH99 alloy (GH99) surface to prepare a (Cu, Ni) solid solution layer. By varying the cladding temperatures, (Cu, Ni) solid solution layers with different Ni contents were achieved. The vacuum cladding process was then followed by vacuum brazing of the Cu-coated GH99 to transparent polycrystalline Al 2 O 3 (TPA). Typical microstructure of the TPA/Cu-cladding GH99 brazed joint was characterized. The effects of different cladding temperatures on microstructural evolution and mechanical response of the brazed joints were discussed. By varying the cladding temperature, different thickness of the reaction layer at the braze filler/TPA interfaces can be achieved, which shows a strong correlation with the mechanical performance of the brazed joint. The maximum shear strength of the brazed joint reached 103 MPa when the cladding temperature was 1105 ºC. Compared with the directly brazed joint, shear strength was improved by 472%.

Introduction

Transparent ceramics possess combined properties of ceramics and transparent materials. In addition to sound transmission of light and wave, transparent ceramics also have high thermal and corrosion resistance, high strength and hardness, and excellent chemical stability [1 ~ 3]. Good mechanical properties have made transparent ceramics distinctive candidates for many optical applications. Transparent polycrystalline Al_2O_3 (TPA) is a traditional transparent ceramic [4], which has been showing broad application potentials in transparent armors, electromagnetic windows, envelopes of high-pressure halide lamps, etc. [1]. Fabrication of these products needs a reliable joining of TPA to metal components. GH99 is a nickel-based superalloy with high strength and excellent oxidation resistance. Joining of transparent Al_2O_3 to GH99 is especially significant for fabricating visors or protective windows.

Because most ceramics have high melting points, brazing is the most suitable method to join ceramics [5 ~ 7]. Up to now, there are only a few researches on the brazing of transparent ceramics. S. Gambaro et al. [8, 9] brazed transparent YAG to Ti6Al4V with various fillers, including AgCuTi, AgCu, and Ag. They held that a thin and continuous metal-ceramic layer containing Ti formed in contact with the YAG, which ensured a sound interfacial adhesion and joining property. Liu et al. [10] successfully brazed transparent alumina and TiAl alloy by using an AgCuTi filler. Their results showed that a continuous reaction layer with a thickness of 1 μm formed at the transparent Al_2O_3 side. The reaction layer was composed of (Cu, Al)$_3$Ti$_3$O single phase. This interfacial reaction layer was lack of Ti-O compound, which was different from the interfacial reaction layers on traditional alumina[11, 12]. Transparent alumina had also been brazed with Ti-based alloy by Li et al. [13] and Benedetti et al. [14]. But detailed discussions about the interfacial reactions of the transparent alumina were not given by them.

Researches on the brazing of normal Al_2O_3 ceramics can provide us some references. R. Arroyave et al. [15] brazed Al_2O_3 ceramic with dissimilar metal substrates. They investigated the nature of the thermochemical interactions between the metal substrates (Fe and Ni) and Cu-Ti filler and found that both metal substrates decreased the chemical activity of Ti in the Cu-Ti filler. Such phenomenons are

widely explained as follows [15, 16]: interreaction between metal element M and Ti decreases the chemical activity of Ti. Then chemical reactions between Al_2O_3 and Ti are weakened. A similar conclusion had also been given by Valette C. et al. [17] They suggested that in the alumina/AgCuTi/CuNi system, Cu and Ni in the CuNi substrate could severely dissolve into the brazing seam during the brazing process. A strong Ni-Ti interaction would lead to Ti being trapped as Ni_3Ti compounds, which would dramatically decrease the activity of the reaction between Ti and alumina. The weak interaction between Ti and alumina led to the formation of an extremely thin reaction layer [17].

These studies can give us some enlightenment that the activity of Ti has a significant effect on the interfacial reaction degrees. Namely, the type and thickness of an interfacial reaction layer can be controlled by varying the activity of Ti. The mechanical strength of a brazed joint can thus be regulated because the type and thickness of the reaction layer at the ceramic side have been widely agreed to be a critical point in the ceramic/metal brazed joints. In view to this, our investigations aim at preparing (Cu, Ni) solid solution (named as (Cu, Ni) for convenience) layers with different Ni content on the surface of GH99. By varying the Ni content in the (Cu, Ni) layer, the chemical activity of Ti in the brazing seam is expected to be adjusted. In our study, pure Cu was cladding on GH99 at different temperatures in vacuum. During cladding, Ni would diffuse from GH99 to the Cu melt. Because Ni has an increased solid solubility in Cu with the increase of temperature, (Cu, Ni) solid solution layers with different Ni content were achieved. The cladding process was followed by brazing the cladded GH99 with TPA. The relationship between microstructure and mechanical properties of the brazed joint was studied in detail.

2. Experimental Procedures

TPA and GH99 used in our experiments were commercially obtained. The transparent Al_2O_3 was polycrystalline, with an average grain size of 20 μm. GH99 was an aging strengthed Ni-based superalloy. The chemical composition of GH99 is listed in Table 1. Cr, Co, W, Al, and Mo are the main alloying elements in the GH99.

Table 1
Chemical composition of the GH99 (wt.%)

Element	C	Si	Mn	Co	Cr	Fe	W	Mo	Al	Ti	Ni
Composition	0.04	0.13	0.12	6.42	6.42	0.54	6.02	3.83	2.05	1.21	et al.

Pure Cu foils with a thickness of 200 μm were used to prepare the (Cu, Ni) cladding layers on the GH99 plates. Before the cladding process, GH99 was wire cut to 16 mm × 8 mm × 2.5 mm plates. The Cu foils were cut to the same size as the GH99 plates. Surfaces of the GH99 plates and Cu foils were polished by abrasive papers up to grid 1000. Then a Cu foil was carefully put on a GH99 plate and was sent into a vacuum furnace with a vacuum degree of 5×10^{-3} Pa. The samples were heated to different peak temperatures (varying from 1090 ºC to 1150 ºC).

It should be noted that the melting point of Cu is 1083 ºC. Therefore, the Cu foils could totally melt at the peak temperatures. The samples were held at the peak temperatures for 1 min in order to make sure that the actual temperatures reach the set temperatures. Then the samples were furnace cooled down. The cladding process is illustrated in Fig. 1 (a).

In the brazing process, TPA was first cut to 5 mm × 4 mm × 3 mm blocks. The 5 mm × 4 mm surface was chosen as the brazing surface. AgCuTi foils and all the brazing surfaces of the TPA and cladded GH99 were polished up to grid 400. The cladded GH99 was then assembled with a TPA block and an AgCuTi foil, as shown in Fig. 1 (b). The assemblies were then sent into the vacuum furnace and were heated at 860 ºC for 10 min under a vacuum of 5×10^{-3} Pa.

Cross-sections of the (Cu, Ni) cladding layers and the brazed joints were characterized by an Empyrean X-ray diffraction (XRD), and a Quanta 200FEG scanning electron microscope (SEM) equipped with an energy dispersive X-ray spectroscopy (EDS). To analyze the interfacial products adjacent to the TPA, the focus ion beam (FIB) technique was conducted by an EFI HELIOS NanoLab 600i focused ion/electron double beam electron microscopy at the interface between the TPA and the braze. Detailed FIB sample preparation processes have been depicted by Xu et al. [18]. Then the FIB sample was observed by a Talos F200X field emission transmission electron microscopy (TEM). Shear tests were conducted by an Instron-5569 electronic universal testing machine, with a head movement speed of 0.5 mm/min. The shear test process is illustrated in Fig. 1 (c). Each shear strength was determined by average the data from three shear samples.

3. Results And Discussion

3.1 Microstructure of the (Cu, Ni) cladding layer

Figure 2 (a) shows the microstructure of the GH99 cladded by a Cu foil at 1090 °C. As depicted in the upper side of Fig. 2 (a), the cladding layer was free of any solidifying defect. According to EDS results listed in Table 2, the cladding layer is mainly composed of (Cu, Ni) solid solutions (see Point A) and Cr(s.s) (see Point B). The Cr(s.s) only distribute in the grain boundaries of the (Cu, Ni). At the interface between the cladding layer and GH99, an interfacial diffusion layer can be seen. The interfacial layer is enlarged in the inset of Fig. 2 (a). Alloying elements of the GH99, such as W and Co were largely accommodated in this layer.

To clarify the formation mechanism of the (Cu, Ni) and Cr (s.s) phases in the cladding layer, binary phase diagrams of Cu-Cr and Cu-Ni are exhibited in Fig. 2 (b) and (c). According to the Cu-Ni phase diagram, Ni can completely dissolve both in the solid Cu and the liquid Cu. In addition, Cr also exhibits high solubility in Cu liquid. A high solubility will induce a significant dissolution of a solid metal into a molten metal, which has been discussed by R. Arroyave [15]. So it can be expected that when in contact with the Cu liquid, Ni and Cr in GH99 would largely dissolve to the Cu melt. In addition, it can be seen from the Cu-Cr binary diagram that Cu and Cr can form a eutectic liquid phase at 1076.6 °C (see Fig. 2 (b)). The solidus

of Cu-Cr binary alloy is lower than the Cu-Ni alloy (above 1084.87 °C), seen Fig. 2 (c). Hence during the solidifying process, (Cu, Ni) solidified firstly, followed by the solidification of the Cu-Cr binary alloy. During the eutectic solidification of the Cu-Cr system, the Cu-Cr system was seperated to a Cu-rich solid solution and a Cr-rich solid solution. Therefore, the Cr-rich solid solution is observed to distribute in the grain boundaries of the (Cu, Ni), as shown in Fig. 2 (a).

Table 2
EDS chemical analysis (at.%) of different positions in Fig. 2 (a)

Spots	Cr	Co	Ni	Cu	W	Possible phase
A	-	-	7.4	92.6		(Cu, Ni)
B	96.1	3.9	-	-		Cr(s,s)

The Ni atoms of the (Cu, Ni) were dissolved from the GH99 to the cladding layer. Hence the Ni content in the (Cu, Ni) could be affected by the degree of the dissolution of Ni. Figure 2 (d) enlarges the Cu-Ni binary phase diagram in the temperature range of 1000 °C ~ 1200 °C and the composition range of 0 wt.%Ni ~ 20 wt.%Ni. At 1090 °C, the maximum solubility of Ni in Cu liquid phase is only about 1.5 at.%. The dissolution of Ni to the melted Cu is faint at this temperature. Raising the cladding temperature (to 1120 °C or 1150 °C) can improve the maximum solubility of Ni, as shown in Fig. 2 (d). Therefore, in order to vary the Ni content in the (Cu, Ni) cladding layer and investigate its effect on microstructure and mechanical strength of the brazed joint, the (Cu, Ni) cladding layers were prepared at different temperatures (from 1090 °C ~ 1150 °C). EDS analysis was conducted on different locations of the surfaces of the achieved (Cu, Ni) layers. According to the EDS results depicted in Fig. 2 (e), the Ni content in the (Cu, Ni) cladding layer increased from 7 at.% to 22 at.% when the temperature was raised from 1090 °C to 1150 °C.

3.2 Typical microstructure of TPA/(Cu, Ni)-GH99 brazed joint

GH99 cladded by Cu foil at 1090 ºC for 1 min (Ni concentration in the cladding layer was 7 at.%) was brazed with TPA by a 50 μm AgCuTi foil at 860 °C for 10 min. A typical microstructure of TPA/(Cu, Ni)-GH99 brazed joint is revealed in Fig. 3. Figure 3 (a) gives the integral microstructure of the brazed joint. TPA and the (Cu, Ni) cladding layer were tightly joined, and the joint was free of voids or cracks. The brazing seam is further magnified in Fig. 3 (b). Three phases comprise the brazing seam. EDS results of the three phases are listed in Table 3. The white (Point A) and the light grey (Point B) phases mainly contain Ag and Cu elements, respectively, which indicates that they are Ag-based and Cu-based solid solutions. Additionally, it is notable that some small dark grey blocks appear near the (Cu, Ni) cladding layer (point C), which are speculated as Cu-Ni-Ti ternary compound according to EDS analysis. The Cu-Ni-Ti ternary compound is further verified to be $CuNi_2Ti$ intermetallic by XRD analysis, see Fig. 4. The formation of $CuNi_2Ti$ intermetallic has also been found in the research of A. A. A. Atiyah et al. [19], in whose research they prepared NiTiCu alloys by powder metallurgy at 850 ºC. The interface between the

TPA and the braze is further magnified in Fig. 3 (c). It can be seen that a thin interfacial layer was generated. In order to analyze the crystal structure of the reaction layer, the joint was immersed into a nitric acid solution to etch the braze filler off and expose the reaction layer on the TPA. Then the reaction layer was characterized by XRD analysis. XRD results in Fig. 4 suggest that the reaction layer is composed of Cu_3Ti_3O and Ni_2Ti_4O. It should be noted that Cu_3Ti_3O and Ni_2Ti_4O have a similar crystal structure. Hence it is not very easy to distinguish these two phases merely by the XRD results. A detailed interface characterization was conducted by TEM analysis.

Table 3
EDS chemical analysis (at.%) of different positions in Fig. 3

Spots	Al	Ag	Ti	Cr	Co	Ni	Cu	Possible phase
A	-	88.9	-	-	-	-	11.1	Ag(s,s)
B	2.8	2.6	-	-	-	-	94.6	Cu(s,s)
C	-	-	30.7	-	-	29.6	39.7	$CuNi_2Ti$
D	26.9	-	39.6	6.6	2.5	13.7	10.7	$Cu_3Ti_3O + Ni_2Ti_4O$

HAADF image of the TPA/braze interface is exhibited in Fig. 5 (a). Figure 5 (b)~(f) show the map distributions of Al, O, Cu, Ni, and Ti elements. It can be recognized that O, Cu, Ni, and Ti elements comprised the interfacial layer. Because Ti has significant tendencies to react with Al_2O_3, the existence of Ti in the interfacial layer indicates that interfacial reactions happened. The bright-field image of the reaction layer is revealed in Fig. 5 (g). Selected area electron diffraction (SAED) patterns of the TPA and the reaction layer are depicted in Fig. 5 (h) and (i). From the Fig. 5 (h) a hexagonal Al_2O_3 phase can be indexed. As for the SAED patterns of the reaction layer, a cubic Cu_3Ti_3O phase (with a lattice parameter of a = 11.258 A) or a cubic Ni_2Ti_4O phase (with a lattice parameter of a = 11.32 A) can be indexed. Cu_3Ti_3O has been largely reported to be a typical reaction product in the AgCuTi/Al_2O_3 brazing system [11, 12]. Also, Ni_2Ti_4O has also been detected by C. G. Zhang et al. [20] in the Al_2O_3/Kovar brazed joint. In our study, both Cu and Ni elements evenly distribute in the reaction layer (see Fig. 5 (d) and (e)). So this interfacial layer is a two-phase structure. It can be inferred that the Cu_3Ti_3O and the Ni_2Ti_4O formed a secondary solid solution by a mutual substitution between Cu and Ni. For convenience, these interfacial reaction phases are denoted as $Cu_3Ti_3O + Ni_2Ti_4O$ in the following discussions.

As shown in Fig. 6 (a), there is also a 20 nm ultra-thin layer well between the TPA and the $Cu_3Ti_3O + Ni_2Ti_4O$ layer. This ultra-thin layer is further magnified in an HRTEM image, see Fig. 6 (b). HRTEM image of the interface between the ultra-thin layer and the TPA is FFT transferred to diffraction patterns, as depicted in the inset of Fig. 6 (b). From the diffraction patterns, two phases can be indexed, which are the hexagonal alumina and the hexagonal Ti_2O_3. It also can be found from the diffraction patterns that the alumina and the Ti_2O_3 phases follow a particular orientation, which is

$$(1\bar{1}2)_{Ti_2O_3[110]}//(102)_{Al_2O_3[2\bar{2}\bar{1}]}$$

Interplanar spacings of (112) crystal face in Ti_2O_3 phase and (102) crystal face in Al_2O_3 are 3.739 Å and 3.479 Å, respectively. Hence the corresponding misfit of the $(112)_{Ti_2O_3}$ and the $(102)_{Al_2O_3}$ interface is 6.95%. The great small mismatch indicates the formation of a semi-coherent interface between Ti_2O_3 and Al_2O_3. Phase interface with lower misfit has lower interface energy. It can be inferred that the Ti_2O_3 phase tends to generate on TPA with a favored orientation to decrease the interface energy. Many other pieces of research have reported the formation of Ti-O compounds at the Al_2O_3/Braze interface. However, the types of proposed Ti-O compounds are different from our study. Characterizations of Ti2O [21], Ti3O2 [22], and TiO [23] have largely been reported. But these reports mainly focus on the brazing of Al_2O_3 ceramic to itself. In our investigation, transparent Al_2O_3 was brazed with a dissimilar Ni-based metal. Moreover, the Ni-based metal was covered by a (Cu, Ni) layer in advance of brazing. During brazing, Ni atoms diffused from the (Cu, Ni) layer into the brazing seam. Because Ni has much stronger interactions with Ti [15], Ni would decrease the chemical activity of Ti. Thus, the interfacial reaction between Ti and TPA was weakened, and Ti_2O_3 with a lower degree of Ti (compared with Ti2O, Ti3O2, or TiO) was formed. This phenomenon is also shared by R. Voytovych et al. [24]. In their research, Ag-Cu-Ti fillers with different Ti content were applied to wet Al_2O_3 ceramic. They found that as Ti content decreased, the Ti-O compound with a lower degree of Ti would form at the interface.

In addition, specific orientations between Ag and Al_2O_3 can be found.

When $[110]_{Ag}//[2\bar{2}\bar{1}]_{Al_2O_3}$, there are two specific orientations: $(1\bar{1}0)_{Ag}//(0\bar{1}2)_{Al_2O_3}$ and $(002)_{Ag}//(102)_{Al_2O_3}$. The specific orientations can also be seen in Fig. 7 (c). Researches have revealed that Ag has a poor wetting property on Al_2O_3 ceramics, and it is hard for Ag to directly bond with Al_2O_3 [25]. But in our study, Ag can cluster on TPA at some specific positions, where preferred orientations exist. From the analysis above, both Ag particles and Ti_2O_3 layer generate on the TPA, following orientation growth mechanisms.

From the HAADF images shown in Fig. 7 (a) and Fig. 8 (a), it can be seen that the grain boundaries of the Cu_3Ti_3O + Ni_2Ti_4O reaction layer exhibit a relatively bright color. It indicates that heavy metal elements have gathered in the grain boundaries. The elements include Ni, Co, and Cr, which can be confirmed by map distribution images given in Fig. 8 (b)~(d). Grain boundaries are the most common short-circuiting paths for diffusion [26]. Hence grain boundary diffusion can be orders of magnitude faster than diffusion through a grain. Hence it can be inferred that the Cu_3Ti_3O + Ni_2Ti_4O reaction layer formed firstly, followed

by the diffusion of Ag and other alloying elements through the intergranular diffusion paths. Ag atoms then cluster at some particular positions at the $Cu_3Ti_3O + Ni_2Ti_4O$ /TPA interface. The other alloying elements including Cr and Co remained in the grain boundaries of the $Cu_3Ti_3O + Ni_2Ti_4O$ reaction layer.

M. Ali et al. [11] have characterized the formation of a γ-TiO layer inside a Cu_3Ti_3O layer in the Al_2O_3/Ag-Cu-Ti/ Al_2O_3 brazing system. They suggested that the formation of the γ-TiO layer is due to the diffusion of Ti atoms through the Cu_3Ti_3O reaction layer. Namely, the Cu_3Ti_3O reaction layer formed first, and the γ-TiO layer is then generated by diffusion of Ti. From our analysis, the formation sequence between the Cu(Ni)-Ti-O reaction layer and the Ti-O layer is consistent with the conclusions given by M Ali. et al. [11]. Namely, the $Cu_3Ti_3O + Ni_2Ti_4O$ layer forms firstly, and the Ti-O layer is generated later. Whereas in our brazing system, the Ti_2O_3 phase formed rather than the γ-TiO given by M Ali. et al [11]. This is because Ni can decrease the activity of Ti, which weakens the reaction between TPA and Ti. Accordingly, Ti_2O_3 with a relatively low degree of Ti is generated. In addition, although the intergranular diffusion of Ti is faster than diffusion through a grain. The intergranular diffusion rate is still limited, especially when Ti atoms have to pass through a 1 μm thick $Cu_3Ti_3O + Ni_2Ti_4O$ layer. Accordingly, the Ti_2O_3 layer is much thinner compared with the $Cu_3Ti_3O + Ni_2Ti_4O$ layer.

3.3 Effect of cladding temperature on microstructure and mechanical strength of the TPA/GH99 brazed joint

The GH99 plates cladded by (Cu, Ni) with different Ni content were brazed with TPA. Figure 9 (a)~(d) are the corresponding images of the joints brazed at 860 ºC for 10 min, with the cladding temperatures varying from 1090 ºC to 1150 ºC. Namely, the Ni content of the (Cu, Ni) layer varied from 7 at.% to 22 at.% in Fig. 9 (a)~(d). During the brazing process, the (Cu, Ni) layer would continually dissolve to the brazing seam, which led to a decrease in the thickness of the (Cu, Ni) layer. After cooling down, it can be seen from Fig. 9 that (Cu, Ni) layers remained for all cases. Accordingly, the (Cu, Ni) layer could be a barrier layer that prevented the Ni from severely diffusing from GH99 to the brazing seam.

Microstructures of the brazing seams are further enlarged, as shown in the insets of Fig. 9 (a)~(d). In the brazing seam, the formation of the $CuNi_2Ti$ compound is due to the chemical reaction between Ti and the Ni that dissolved from the (Cu, Ni) layer. For the (Cu, Ni) layer with a higher Ni content, a larger amount of Ni would dissolve from the (Cu, Ni) layer to the brazing seam. Therefore, a more massive amount of Ti would be attracted by the dissolved Cu and Ni elements to form $CuNi_2Ti$ compounds. Hence it can be seen from Fig. 9 (a)~(d) that with the increase of Ni content of the (Cu, Ni) cladding layers, the amount of the $CuNi_2Ti$ in the brazing seam increased as well.

The TPA/braze interfaces of the brazed joints with different Ni contents in the (Cn, Ni) cladding layers are further enlarged in Fig. 10 (a)~(d). When the Ni content was 7 at.% (the cladding temperature was 1090 °C), the thickness of the reaction layer was about 1 μm. When the Ni content was increased to 10 at.% (the cladding temperature was 1105 °C), the thickness dramatically decreased to 0.6 μm. As

discussed above, this phenomenon is mainly induced by the reduction of the activity of Ti. A weak activity of Ti leads to a weak interfacial reaction between Ti and TPA. When the Ni content further increases to 14 at.% (the cladding temperature is 1120 °C), however, the continuity of the reaction layer is destroyed. The formation of the thin and discontinuous reaction layer is caused by a further decrease in the activity of Ti. When the cladding temperature is raised to 1150 °C (the Ni content is increased to 22 at.%), the reaction layer totally disappears, as shown in Fig. 10 (d). Accordingly, the thickness of the interfacial reaction layer could be regulated by varying the activity of the active Ti element.

The TPA and GH99 were also directly brazed by an AgCuTi foil at 860 ºC for 10 min for a comparison purpose. When TPA and GH99 were directly brazed, the significant diffusion of Ni would induce the formation of a mass of intermetallic compounds in the brazing seam, see Fig. 11. EDS results show that the chemical composition of the compound is 76.9 at.% Ni and 23.1 at.% Ti. Therefore, the Ni_3Ti brittle compounds severely aggregate in the brazing seam, which is terrible for relieving the residual thermal stress of the joint. The severe Ni diffusion would weaken the activity of Ti. Hence the reaction between Ti and TPA would be faint. Accordingly, the interfacial layer was not observed at the TPA/braze interface in the inset of Fig. 11. Because of the large amount of the brittle compounds and the poor interfacial bonding, the directly bonded joints exhibited poor mechanical properties. In our experiments, penetrating cracks were observed in all directly bonded samples.

Plenty of researches has suggested that the degree of interfacial reactions could significantly affect the mechanical properties of a brazed joint [27, 28]. Dai et al. [29] investigated the plasticity of the TiO + Cu_3Ti_3O phase. They concluded that the TiO + Cu_3Ti_3O exhibited a high hardness. Moreover, from a load-displacement curve, the elastic recovery of the TiO + Cu_3Ti_3O phase was tested to be 43.1%. Compared with Ag with an elastic recovery of 10.2%, the TiO + Cu_3Ti_3O owns quite a poor plasticity [29]. Thus it can be inferred that in our brazing system, the TPA/braze interfacial reaction phase also exhibited poor plasticity. A too thick brittle interfacial layer is adverse for the joint to relieve the residual interfacial stress.

Whereas if the interfacial reaction layer is quite thin, the bonding between the TPA and the braze is weak. Hence to achieve a maximum mechanical strength of the brazed joint, there should be an optimized thickness of the interfacial reaction layer. As has been discussed, (Cu, Ni) cladding layers with different Ni content could be prepared by cladding Cu foils on GH99 at different temperatures. The varied Ni content of the (Cu, Ni) layers could regulate the activity of Ti. Thus the thickness of the reaction layer between the TPA and the braze could be controlled via the (Cu, Ni) cladding method. Shear strength of the brazed joints without cladding and with different cladding temperatures are given in Fig. 12. With the increase of the cladding temperature, the shear strength of the brazed joints improves then decreases. When the cladding temperature is 1105 °C, the maximum shear strength of the brazed joint is achieved, which is 103 MPa. Compared with the joint brazed without the assistance of the (Cu, Ni) cladding layer, shear strength was improved by 472%. Variation of the mechanical strength is recognized as a result of the regulation of the thickness of the reaction layers by the (Cu, Ni) cladding layer.

Conclusions

In this study, a (Cu, Ni) layer was prepared by cladding a pure Cu foil on GH99. Then TPA and the cladded GH99 were successfully brazed with the assistant of the (Cu, Ni) cladding layer. Interfacial bonding between the TPA and the AgCuTi braze was studied in detail. The influence of the Ni content in the (Cu, Ni) layer on the microstructure and mechanical property of the brazed joint was also investigated. Based on the analysis above, the main conclusions were achieved, which are as follows:

(1) The (Cu, Ni) layer could be successfully prepared by cladding a Cu foil on the surface of the GH99 in vacuum. The cladding layers were mainly composed of the (Cu, Ni) phase. Ni content of the (Cu, Ni) increased with the increase of the cladding temperature. With the cladding temperature raising from 1090 ºC to 1150 ºC, the Ni content of the (Cu, Ni) layer increased from 7 at.% to 22 at.%.

(2) A sound TPA/AgCuTi/GH99 brazed joint could be achieved at 860 ºC for 10 min with the assistance of the (Cu, Ni) cladding layer. In the brazing seam, Ti reacted with Cu and Ni that dissolved from the (Cu, Ni) cladding layer to form the $CuNi_2Ti$ compound. At the TPA/braze interface, Ti reacted with the TPA, leading to the generation of Cu3Ti3O, Ni2Ti4O, and Ti_2O_3 phases. A particular orientation relationship between the Ti_2O_3 and the TPA was detected, which was

$$(1\bar{1}2)_{Ti_2O_3[110]}//(102)_{Al_2O_3[2\bar{2}\bar{1}]}.$$

Typical microstructure of the brazed joint was TPA/Ti_2O_3/Cu_3Ti_3O + Ni_2Ti_4O/Ag(s.s) + Cu(s.s) + $CuNi_2Ti$/(Cu, Ni)/GH99.

(3) The thickness of the TPA/braze interfacial reaction layer correlates with the Ni content of the (Cu, Ni) layer. With the increase of the Ni content of the (Cu, Ni) layer, the chemical activity of Ti decreased due to the strong Ni-Ti interaction. Thus the thickness of the Ti_2O_3 + Cu_3Ti_3O + Ni_2Ti_4O interfacial reaction layer diminished with the increase of the cladding temperature.

(4) The thickness of the reaction layer corresponds to the strength of the brazed joint. By optimizing the Ni content of the (Cu, Ni) layer, the maximum shear strength of the brazed joint was achieved, which was 103 MPa when the cladding temperature was 1105 ºC. Compared with the TPA/AgCuTi/GH99 directly brazed joint, shear strength was improved by 472%.

Declarations

Acknowledgement

The authors gratefully acknowledge the financial support of the National Natural Science Foundation of China (Grant nos.51775142, and 51805113), China Postdoctoral Science Foundation funded project (Grant no. 2018M631923), Fundamental Research Funds for the Central Universities (Grant no.

HIT.NSRIF.2019006), Innovative Research Group Project of the National Natural Science Foundation of China (Grant nos. 51621091).

References

[1] M. Trunec, J. Klimke, Z. J. Shen, Transparent alumina ceramics densified by a combinational approach of spark plasma sintering and hot isostatic pressing, J. Eur. Ceram. Soc. 36 (2016) 4333-4337.

[2] R. Apetz, M. P. B. V. Bruggen, Transparent alumina: A light-scattering model, J. Am. Ceram. Soc. 86 (2003) 480-486.

[3] A. Krell, P. Blank, H. Ma, T. Hutzler, Transparent Sintered Corundum with High Hardness and Strength, J. Am. Ceram. Soc. 86 (2003) 12-18.

[4] A. Krell, T. Hutzler, J. Klimke, Transmission physics and consequences for materials selection, manufacturing, and applications, J. Eur. Ceram. Soc. 29 (2009) 207-221.

[5] Z. W. Yang, C. L. Wang, Y. Han, Y. T. Zhao, Y. Wang, D.P. Wang, Design of reinforced interfacial structure in brazed joints of C/C composites and Nb by pre-oxidation surface treatment combined with in situ growth of CNTs, Carbon 143 (2019) 494-506.

[6] M. Lei, Y. L. Li, H. Zhang, Interfacial microstructure and mechanical properties of the TiC-Ni cermet/Ag-Cu-Zn/Invar joint, Vacuum 168 (2019) 108830.

[7] J. M. Shi, Q. Wang, J. L. Li, J. T. Xiong, L. X. Zhang, J. C. Feng, Interfacial microstructure and mechanical property of ZrC-SiC ceramic and TiAl joint brazed with Ag-Zf active filler metal, Mater. Charact. 156 (2019)

[8] S. Gambaro, F. Valenza, A. Passerone, G. Cacciamani, M. L. Muolo, Brazing transparent YAG to Ti6Al4V: activity and characterization, J. Eur. Ceram. Soc. 36 (2016) 4185-4196.

[9] S. Gambaro, M. L. Muolo, F. Valenza, G. Cacciamani, L. Esposito, A. Passerone, Wettability of transparent YAG (Y3Al5O12) by molten Ag–Cu–Ti alloys, J. Eur. Ceram. Soc. 35 (2015) 2895-2906.

[10] X. P. Liu, L. X. Zhang, Z. Sun, J. C. Feng, Microstructure and mechanical properties of transparent alumina and TiAl alloy joints brazed using Ag-Cu-Ti filler metal, Vacuum 151 (2018) 80-89.

[11] M. Ali, K. M. Knowles, P. M. Mallinson, J. A. Fernie, Interfacial reactions between sapphire and Ag–Cu–Ti-based active braze alloys, Acta Mater. 103 (2016) 859-869.

[12] M. Ali, K. M. Knowles, P. M. Mallinson, J. A. Fernie, Microstructural evolution and characterisation of interfacial phases in Al_2O_3/Ag–Cu–Ti/Al_2O_3 braze joints, Acta Mater. 96 (2015) 143-158.

[13] C. Li, X. Q. Si, L. Chen, J. L. Qi, Z. G. Liu, Y. X. Huang, Z. B. Dong, J. C. Feng, J. Cao, Non-destructive measurement of residual stress distribution as a function of depth in sapphire/Ti6Al4V brazing joint via Raman spectra, Ceram. Int. 45 (2019) 3284-3289.

[14] A. Benedetti, S. Gambaro, F. Valenza, M. Faimali, M. Colli, J. Hostasa, M. Delucchi, Ag and AgCu as brazing materials for Ti6Al4V-Y3Al5O12 joints: Does ennoblement affect the galvanic behaviour in seawater?, Electrochim. Acta 283 (2018) 155-166.

[15] R. Arroyave, T. W. Eagar, Metal substrate effects on the thermochemistry of active

brazing interfaces, Acta Mater. 51 (2003) 4871-4880.

[16] N. Eustathopoulos, R. Voytovych, The role of activity in wetting by liquid metals: a review, J. Mater. Sci. 51 (2016) 425-437.

[17] C. Valette, M. Devismes, R. Voytovych, N. Eustathopoulos, Interfacial reactions in alumina/CuAgTi braze/CuNi system, Scr. Mater. 52 (2005) 1-6.

[18] J. K. Xu, C. X. Wang, X. L. Ji, Q. An, Y. H. Tian, T. Suga, Direct bonding of high dielectric oxides for high-performance transistor applications, Scr. Mater. 178 (2020) 307-312.

[19] A. A. Atiyah, A. A. K. A. Ali, N. M. Dawood, Characterization of NiTi and NiTiCu Porous Shape Memory Alloys Prepared by Powder Metallurgy (Part I), Arab. J. Sci. Eng. 40 (2015) 901-913.

[20] C. G. Zhang, G. J. Qiao, Z. H. Jin, Active brazing of pure alumina to Kovar alloy based on the partial transient liquid phase (PTLP) technique with Ni–Ti interlayer, J. Eur. Ceram. Soc. 22 (2002) 2181-2186.

[21] J. J. Stephens, F. M. Hosking, T. J. Headley, P. F. Hlava, F. G. Yost, Reaction layers and mechanisms for a Ti-activated braze on sapphire, Metall. Mater. Trans. A-Phys. Metall. Mater. Sci. 34A (2003) 2963-2972.

[22] K.-L. Lin, M. Singh, R. Asthana, Interfacial characterization of alumina-toalumina joints fabricated using silver–copper–titanium interlayers, Mater. Charact. 90 (2014) 40–51.

[23] S. Mandal, A.K. Ray, A.K. Ray, Correlation between the mechanical properties and the microstructural behaviour of Al_2O_3–(Ag–Cu–Ti) brazed joints, Mater. Sci. Eng. A 383 (2004) 235–244.

[24] R. Voytovych, F. Robaut, N. Eustathopoulos, The relation between wetting and interfacial chemistry in the CuAgTi/alumina system, Acta Mater. 54 (2006) 2205-2214.

[25] J. R. Friant, A. Meier, J. T. Darsell, K. S. Weil, Transitions in Wetting Behavior Between Liquid Ag–CuO Alloys and Al_2O_3 Substrates, J. Am. Ceram. Soc. 95 (2012) 1549-1555.

[26] Y. Amouyal, S. V. Divinski, Y. Estrin, E. Rabkin, Short-circuit diffusion in an ultrafine-grained copper–zirconium alloy produced by equal channel angular pressing, Acta Mater. 55 (2007) 5968-5979.

[27] Z. S. Yu, M. F. Wu, F. J. Wang, Effect of reaction layer thickness on strength of Al2O3/AgCuTi/Ti-6Al-4V brazed joints, Mater. Sci. Technol. 17 (2001) 1441-1443.

[28] Z. W. Yang, C. L. Wang, Y. Han, Y. T. Zhao, Y. Wang, D. P. Wang, Design of reinforced interfacial structure in brazed joints of C/C composites and Nb by pre-oxidation surface treatment combined with in situ growth of CNTs, Carbon 143 (2019) 494-506.

[29] X. Y. Dai, J. Cao, J. Q. Liu, D. Wang, J. C. Feng, Interfacial reaction behavior and mechanical characterization of ZrO_2/TC4 joint brazed by Ag–Cu filler metal, Mater. Sci. Eng. A-Struct. Mater. Prop. Microstruct. Process. 646 (2015) 182-189.

Figures

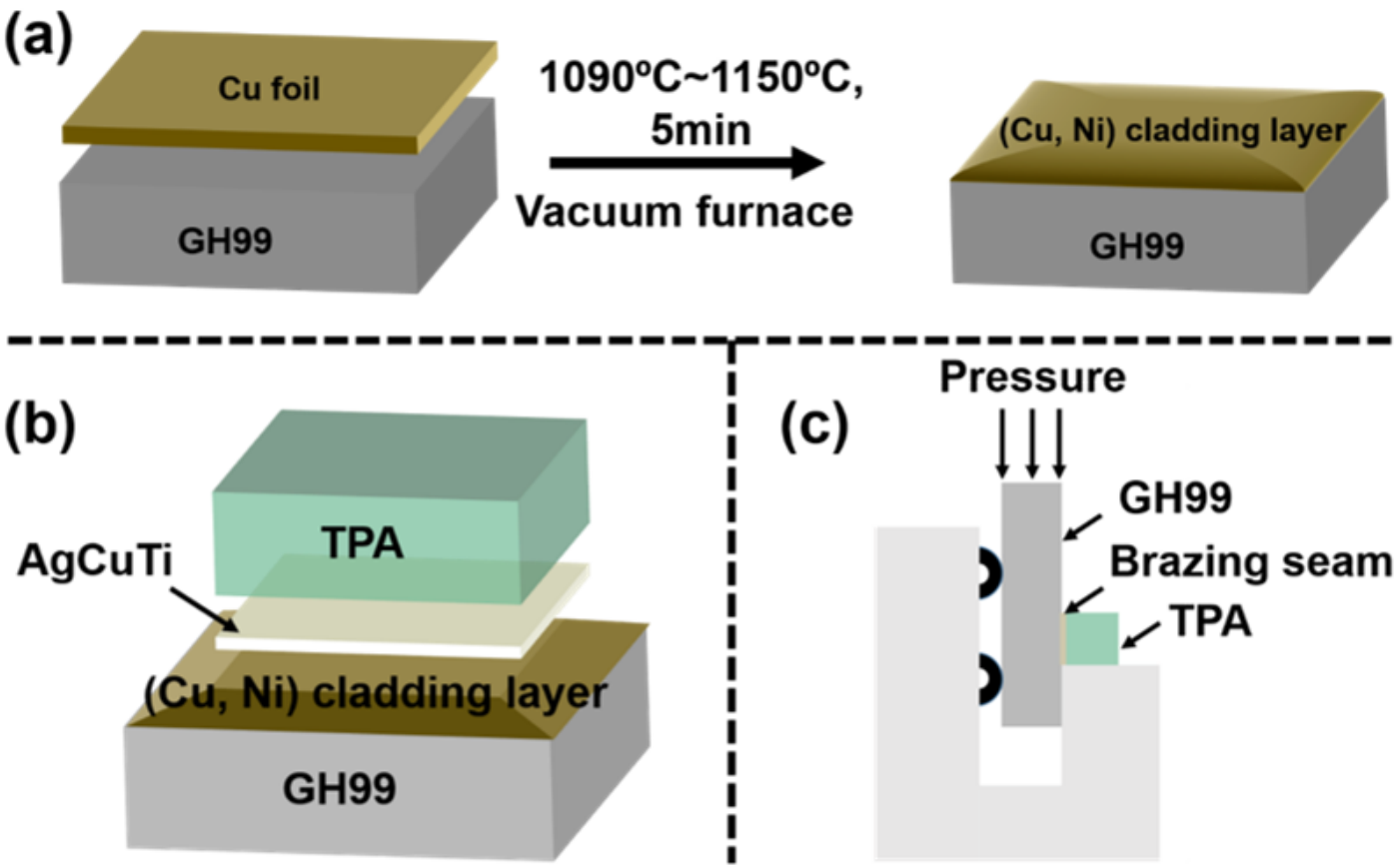

Figure 1

Sketches of (a) the vacuum cladding process, (b) the brazing assembly, and (c) the shear test assembly

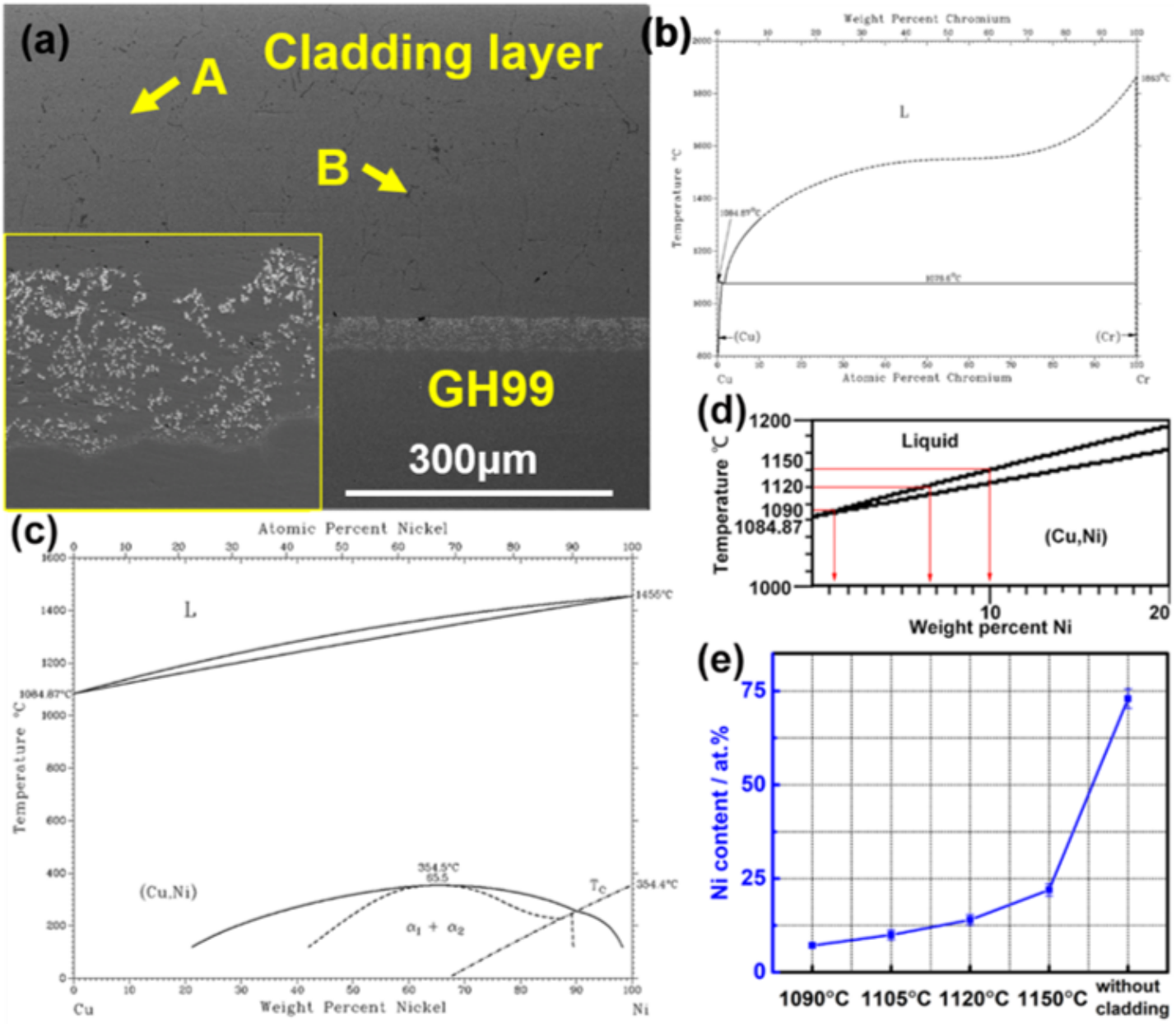

Figure 2

(a) Microstructure of the interface between the cladding layer and GH99; Binary phase diagram of (b) Cu-Cr system and (c) Cu-Ni system; (d) Enlarged Cu-Ni binary phase diagram; (e) Ni content in the (Cu, Ni) cladding layer varying with cladding temperature.

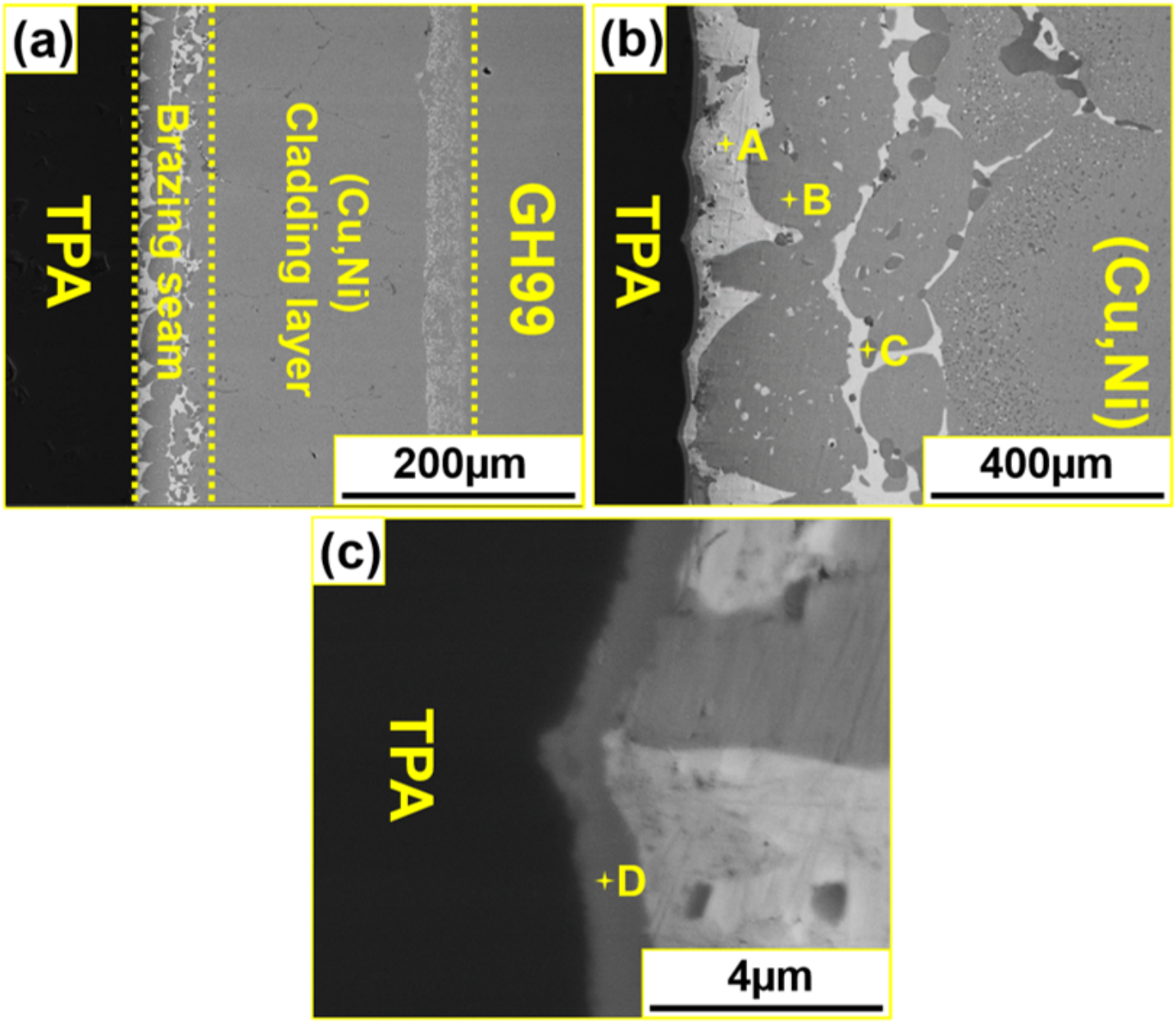

Figure 3

Microstructure of (a) the brazed joint with the assistance of (Cu, Ni) cladding layer, (b) the brazing seam enlarged from Fig. 3 (a), and (c) the TPA/braze interface enlarged from Fig. 3 (b)

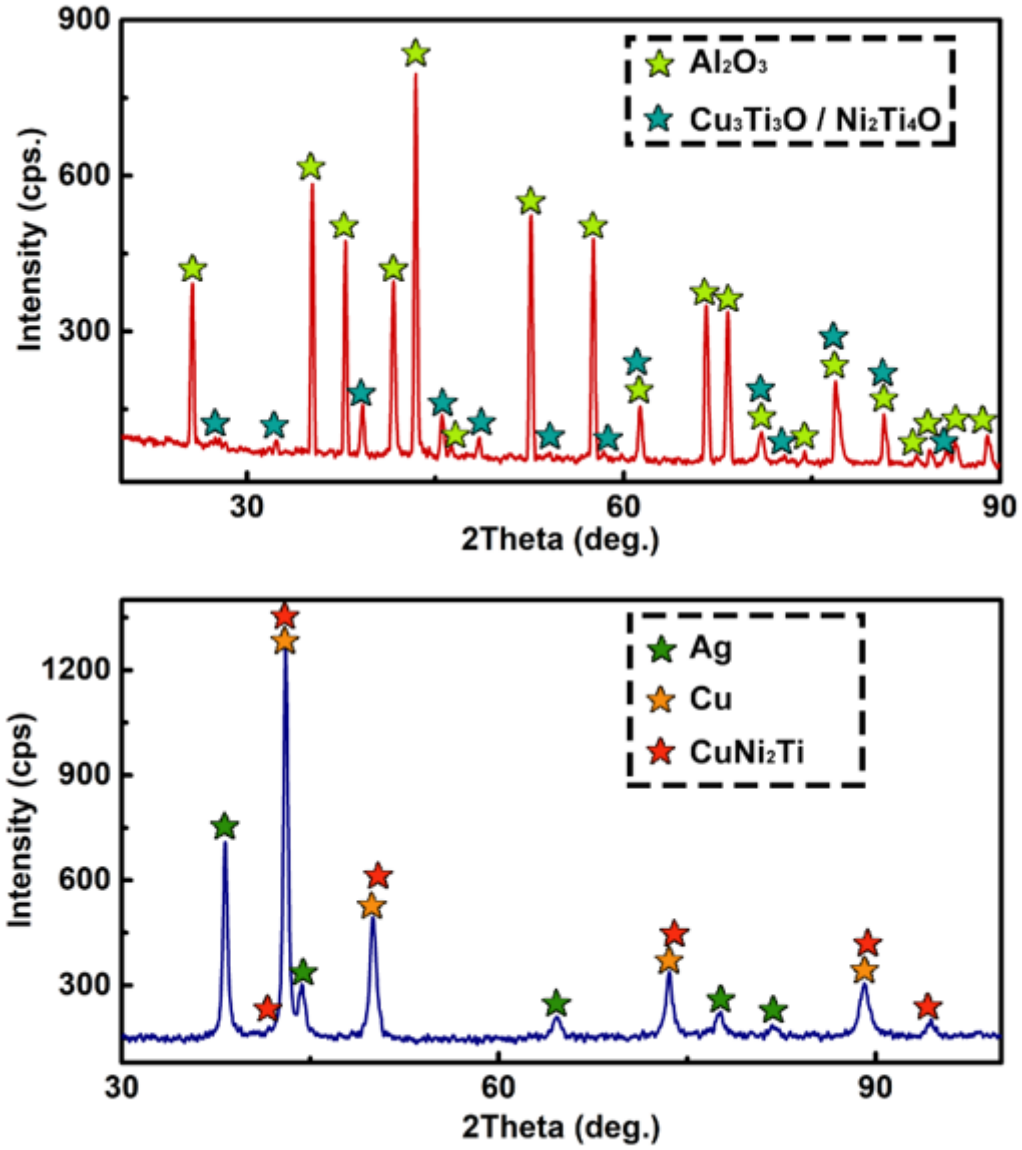

Figure 4

XRD results of (a) the nitric acid solution treated TPA surface and (b) the brazing seam

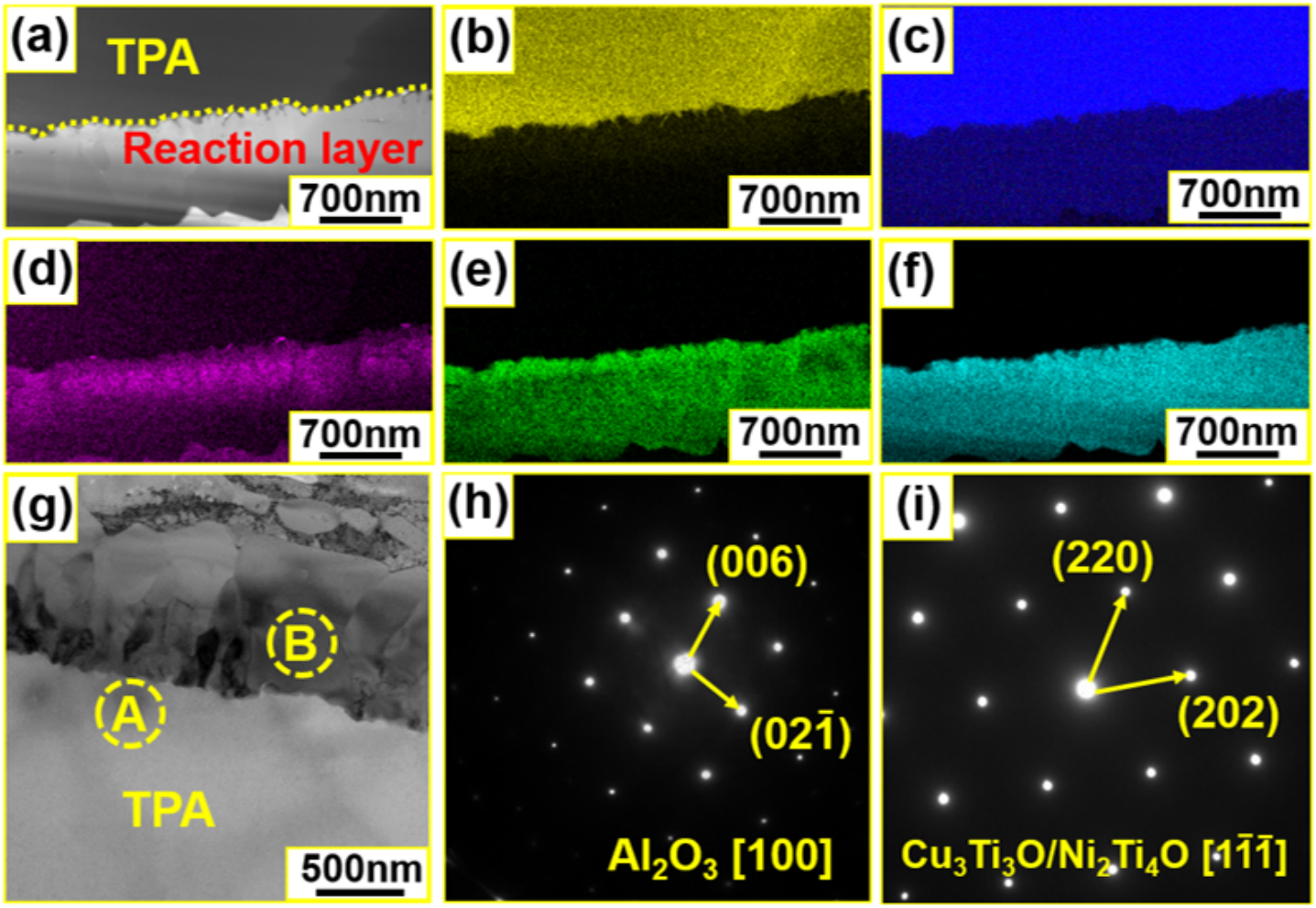

Figure 5

(a) HAADF image of the TPA/braze interface; Map distributions of the (b) Al, (c) O, (d) Cu, (e) Ni, and (f) Ti elements; (g) Bright field image of the TPA/braze interface; SAED patterns of (h) the area A and (i) the area B of the Fig. 5(g).

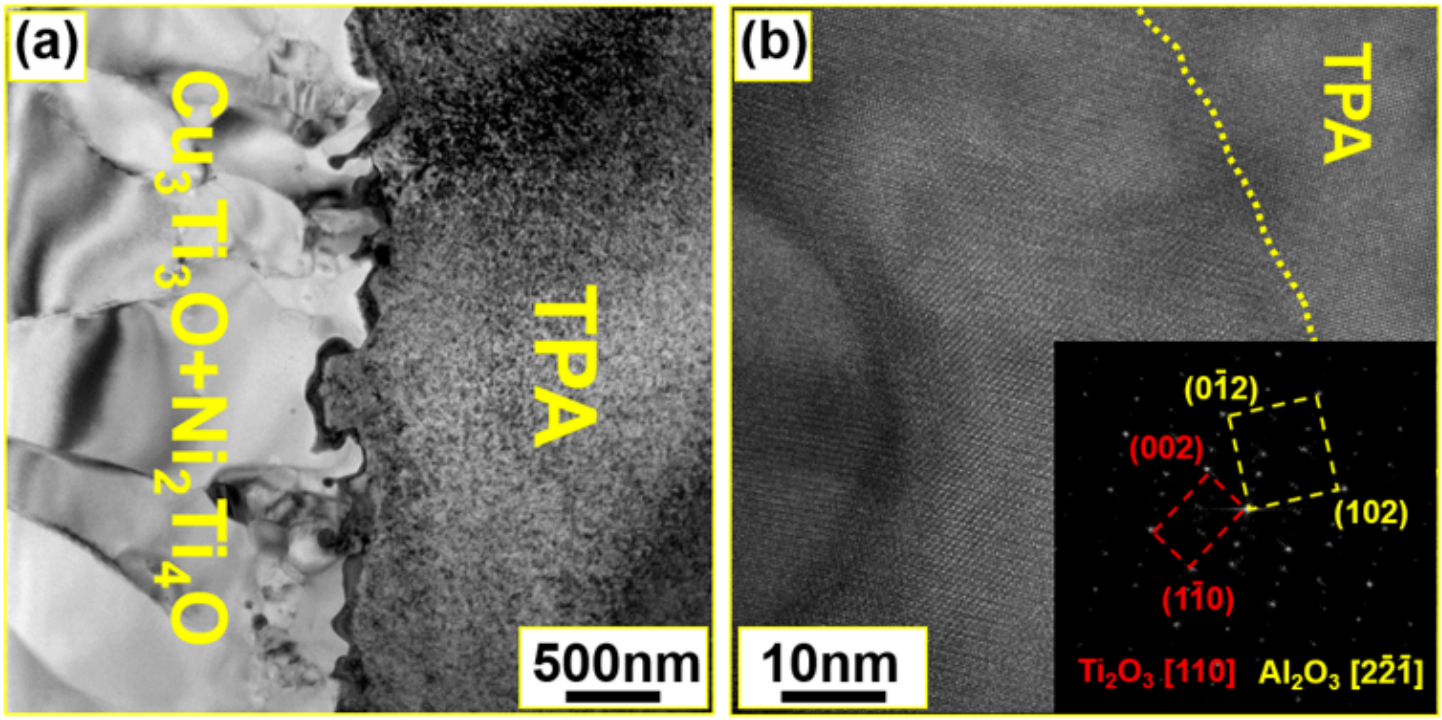

Figure 6

(a) Bright field image of the TPA/Cu3Ti3O+Ni2Ti4O interface; (b) HRTEM image of the Ti2O3 thin layer.

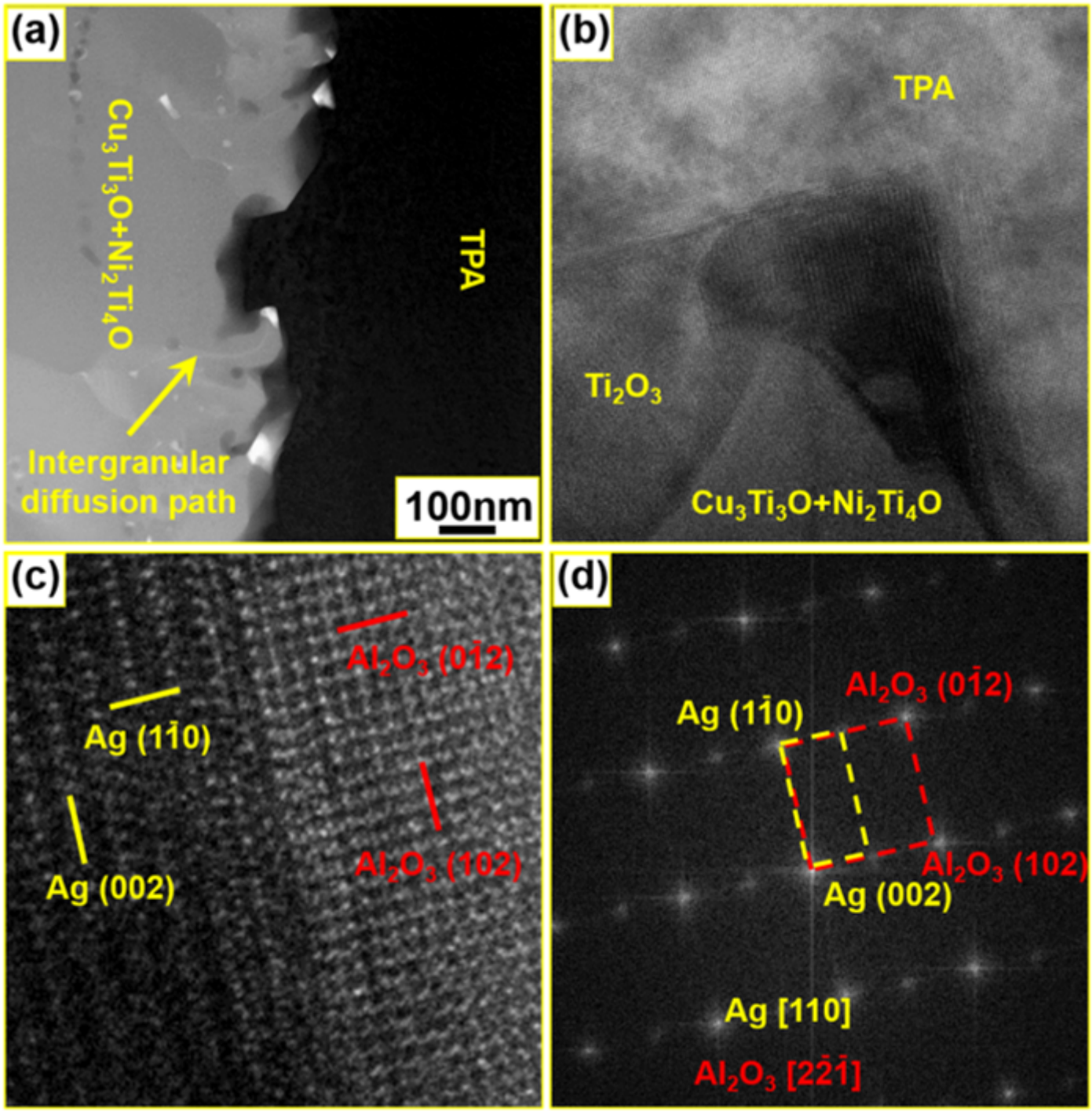

Figure 7

(a) HAADF image of the TPA/Cu3Ti3O+Ni2Ti4O interface; (b) HRTEM image of the Ag nanoparticle (c) Enlarged HRTEM image of the TPA/Ag interface; (d) diffraction patterns transferred from Fig. 7 (c).

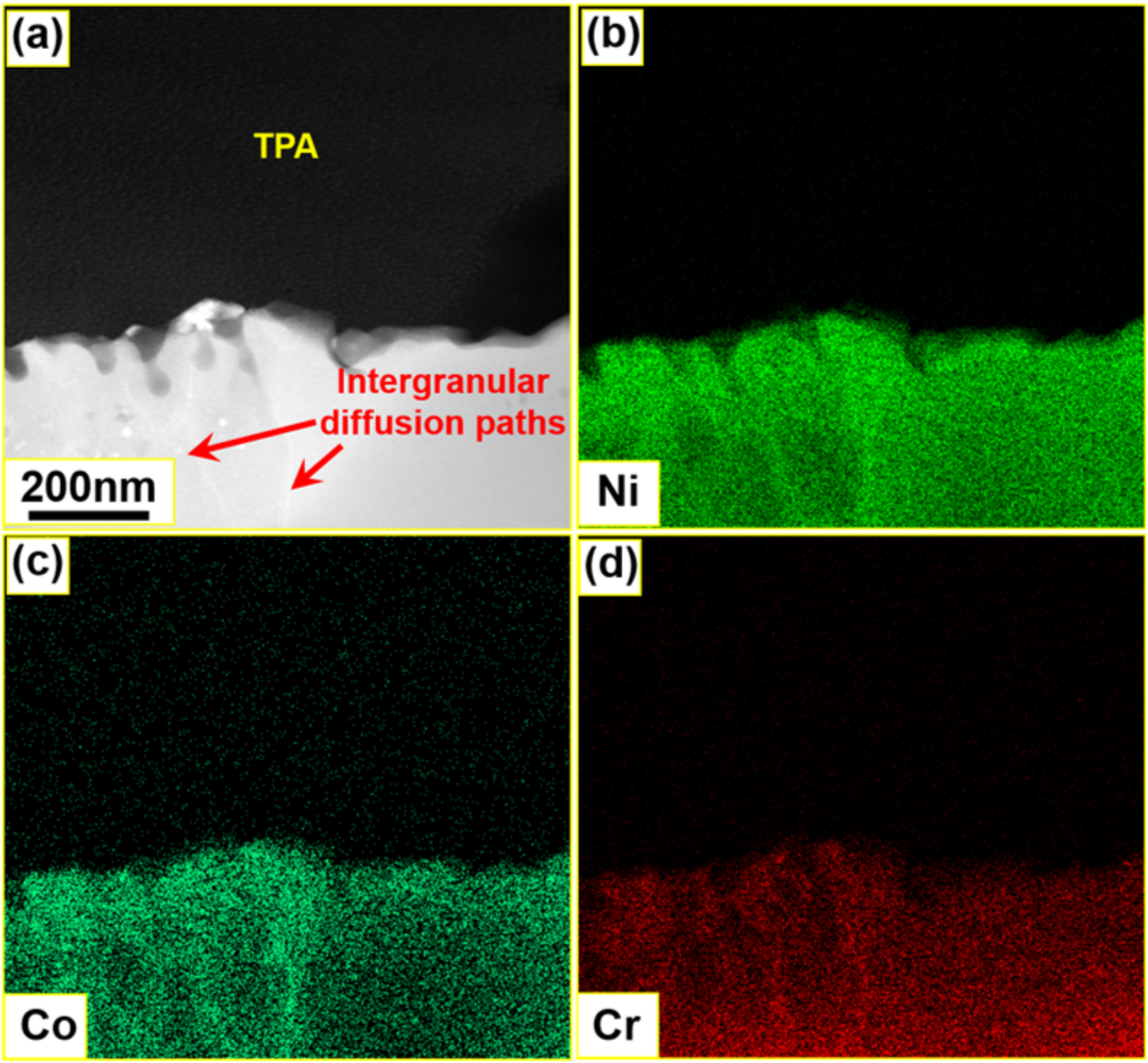

Figure 8

(a) Enlarged HAADF image of the TPA/Cu3Ti3O+Ni2Ti4O interface; Map distributions of the (b) Ni, (c) Co, and (d) Cr elements in Fig. 8 (a).

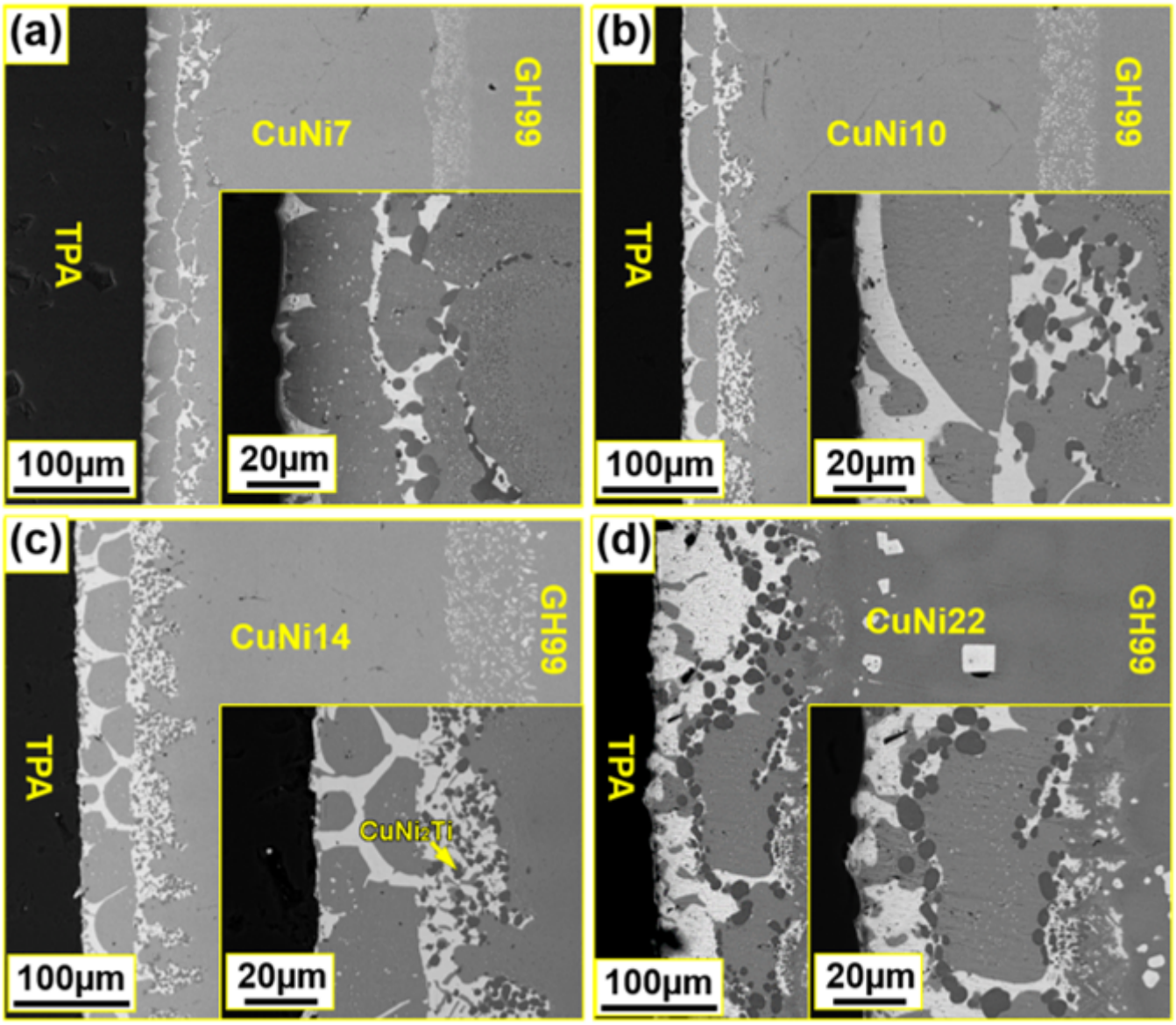

Figure 9

Microstructure of the TPA/GH99 joints brazed with the assitance of the (Cu, Ni) cladding layers prepared at different cladding temperatures: (a) 1090 °C, (b) 1105 °C, (c) 1120 °C, and (d) 1150 °C. (The joint was brazed at 860 °C for 10 min)

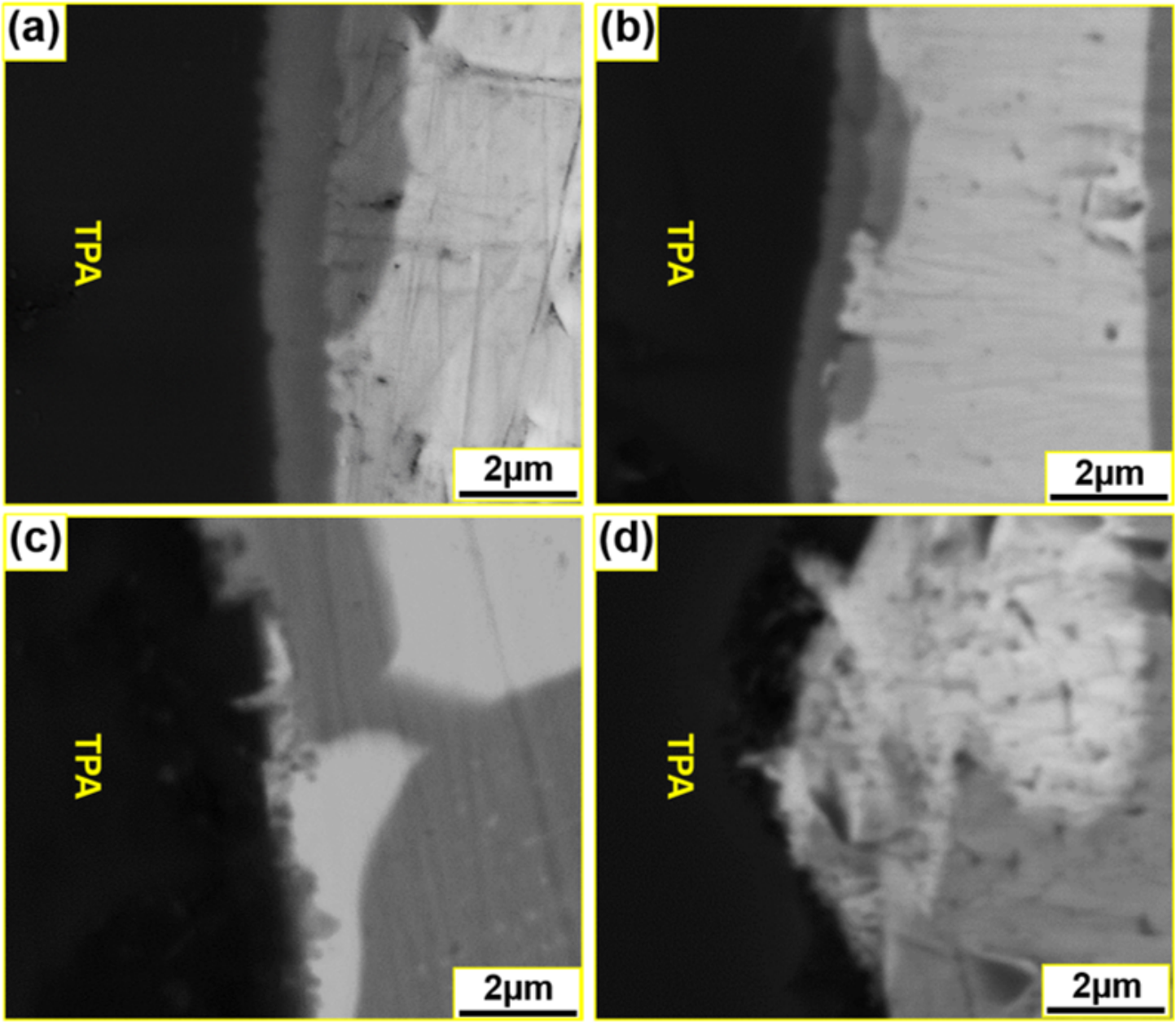

Figure 10

10 Microstructure of the TPA/braze interfaces of the joints brazed with the assitance of the (Cu, Ni) cladding layers prepared at different cladding temperatures: (a) 1090 °C, (b) 1105 °C, (c) 1120 °C, and (d) 1150 °C.

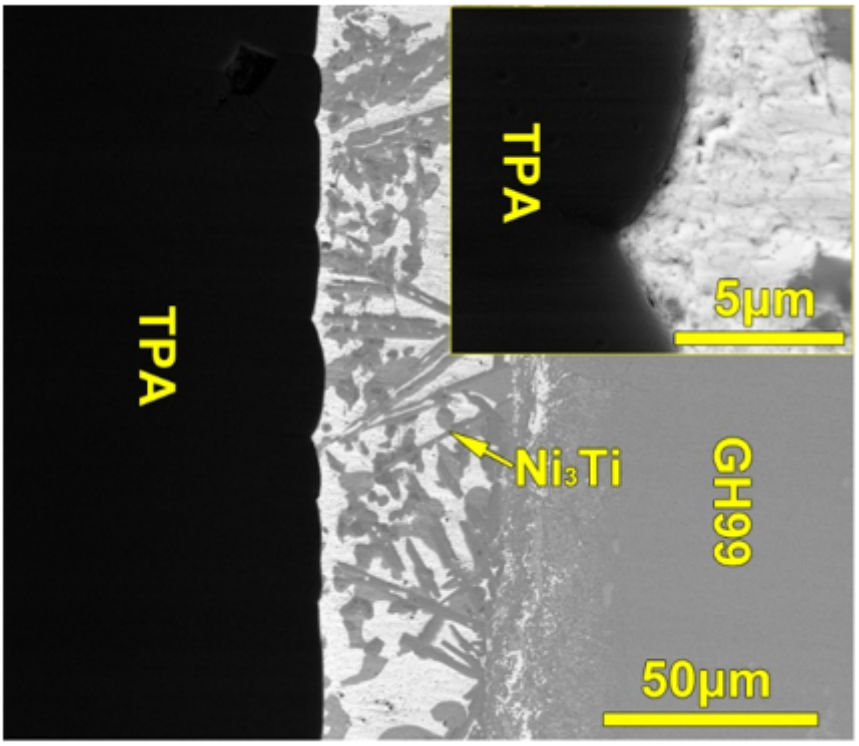

Figure 11

Typical microstructure of the TPA/GH99 joint directly brazed with an AgCuTi foil at 860 °C for 10 min.

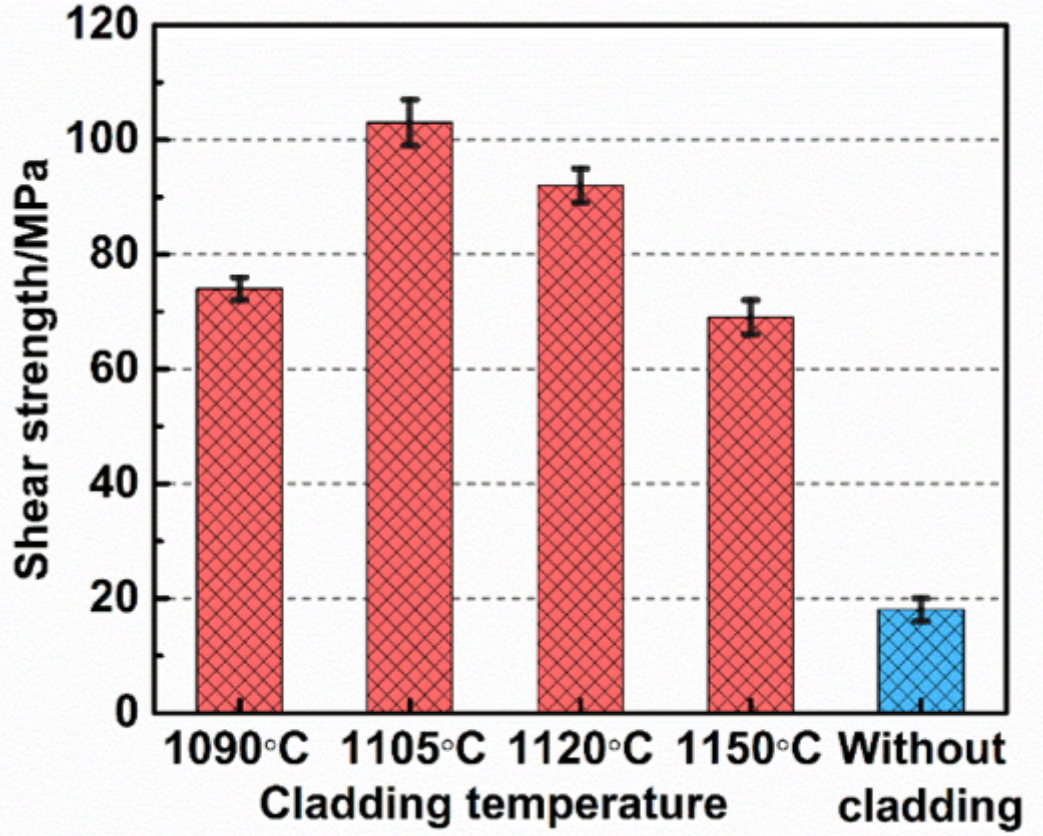

Figure 12

Shear strengthes of the joints brazed with and without the assistant of the (Cu, Ni) cladding layers.